



# N-Doped carbon dots with pH-sensitive emission, and their application to simultaneous fluorometric determination of iron(III) and copper(II)

Rajkumar Bandi<sup>1,2</sup> · Ramakrishna Dadigala<sup>1</sup> · Bhagavanth Reddy Gangapuram<sup>1,3</sup> · Fedlu Kedir Sabir<sup>4</sup> · Madhusudhan Alle<sup>2</sup> · Seung-Hwan Lee<sup>2</sup> · Veerabhadram Guttena<sup>1</sup>

Received: 5 June 2019 / Accepted: 9 November 2019 / Published online: 7 December 2019  
© Springer-Verlag GmbH Austria, part of Springer Nature 2019

## Abstract

Simultaneous fluorometric determination of iron(III) and copper(II) without the use of any masking agent or additional treatment is achieved by using N-doped carbon dots (NCDs). The NCDs were hydrothermally prepared, have strongest excitation/emission peaks at 320/406 nm and a 47% quantum yield. Excitation-tunable emission is found to depend on solution pH values. This supports the involvement of surface states in the origin of the excitation dependent nature. The NCDs were employed as a fluorescent probe for the simultaneous determination of Fe(III) with a linear response in the 3–60  $\mu\text{M}$  concentration range and a 0.31  $\mu\text{M}$  detection limit (LOD). The probe also responds linearly to Cu(II) in the 0.5–15  $\mu\text{M}$  concentration range and with a 56 nM LOD. With the addition of Cu(II), the absorption spectra of NCDs presented a clear decrease in the intensity at 312 nm followed by an increase at 360 nm. This is not observed in the presence of Fe(III). The fluorescence lifetime of NCDs (5.8 ns) is reduced by Fe(III) but not by Cu(II). Thus, the two metal ions can be simultaneously detected without the need for any reagents. The probe was employed to quantify Fe(III) and Cu(II) in spiked water, serum, and urine samples.

**Keywords** Hydrothermal method · pH dependent excitation tuneable emission · Dual metal detection · Ferric ion · Real sample analysis · Fluorescence lifetime · Inner filter effect · Individual ion discrimination · Serum and urine analysis

## Introduction

Copper as well as iron are the two vital nutrient elements [1, 2]. However, surplus intake of these elements can result in

disorders like renal failure, Wilson's, Prion and Alzheimer's diseases [3, 4]. On the other hand, copper and iron are widely used in the agriculture and industry. Hence, the potential toxic effects of these metal ions to human beings from polluted water and soil remain a global challenge. Therefore, the quantification of copper & iron ions in biological and ecological samples is of vital significance in human health monitoring. Even though conventional analytical techniques can be best employed for this, cost and non-portable nature limits their use. Hence, developing reliable, fast and cheap techniques to monitor these metal ions is of great need. With their straightforwardness, operational ease and great sensitivity fluorescence based methods can better serve this purpose [5].

A wide range of fluorescent probes including organic molecules, quantum dots, and metal nanoclusters were explored for the recognition of various metal ions [6]. Among these, carbon dots (CDs) presented great promise. In literature, we can find a huge number of reports on the usage of CDs for the detection of wide variety of metal ions such as Fe(III), Pb(II), Hg(II), Cu(II), Zn(II), Co(II), Ag(I), Au(III), Al(III), and K(I) [7, 8]. Though these methods are effective, the major

---

**Electronic supplementary material** The online version of this article (<https://doi.org/10.1007/s00604-019-4017-1>) contains supplementary material, which is available to authorized users.

---

✉ Veerabhadram Guttena  
gvbhadram@gmail.com

<sup>1</sup> Department of Chemistry, Osmania University, Hyderabad, Telangana State 500007, India

<sup>2</sup> Institute of Forest Science, College of Forest and Environmental Sciences, Kangwon National University, Chuncheon 24341, Republic of Korea

<sup>3</sup> Department of Chemistry, PG Center Wanaparthy, Palamuru University, Mahabub Nagar, Telangana State 509001, India

<sup>4</sup> Department of Applied Chemistry, School of Applied Natural Science, Adama Science and Technology University, 1888 Adama, Ethiopia

shortcoming of these probes lies in their ability to recognize only a single metal ion. Simultaneous detection of multiple metal ions by single probe is more advantageous for the analysis of real samples which usually contain multiple metal ions. In this regard, usage of single CDs probe for the detection of multiple metal ions is gaining much attention. For instance, Wenli Gao et al. have used red emitting CDs for the detection of Pt(II), Au(III) & Pd(II) ions [9]. Xiang Zhu et al. detected Fe(III) & Ag(I) ions using N,S co-doped CDs [10]. Similarly, Guojuan Ren et al. applied NCDs for Hg(II) & Ag(I) detection [11] and Ankit Kumar Singh et al. used N, P doped CDs for Hg(II) & Cr(VI) detection [12]. Even though these probes are sensitive to multiple metal ions they lack the important feature of differentiating individual metal ions.

It is of great difficult to find a probe which can respond to multiple metal ions with selective discrimination of each ion. Either the usage of specific chelating agents to mask one metal ion or the treatment with additional reagents to discriminate each ion is necessary. For instance, Polymer nanodots of g-C<sub>3</sub>N<sub>4</sub> were applied for the detection of Fe(III) & Cu(II) which required the use of sodium hexametaphosphate to mask the effect of Fe(III) ions [13]. Baogang wang et al. employed NCDs for the detection of Hg(II) & Cu(II) in which individual ion discrimination is achieved by using masking agents of P<sub>2</sub>O<sub>7</sub><sup>-4</sup> and S<sub>2</sub>O<sub>3</sub><sup>-2</sup> [14]. Khemnath Patir et al. used ascorbic acid and trisodium citrate to discriminate Hg(II) & Cu(II) [15]. Similarly some researchers used masking effects of different buffers to discriminate the individual ions [16–18].

However, the introduction of an additional reagent complicates the detection process and may cause fluctuations in the emission intensity and interfere with the accuracy of trace level analysis [19]. In this regard, developing a probe which simplifies the process of individual ion discrimination by producing different responses to different ions is of great need. However CDs were less explored in this regard. Vinay sharma et al. used carbon nanoparticles to detect Hg(II) & Pd(II) ions and successfully differentiated them using FL Lifetime (TCSPC) [20]. In our work, both UV-Vis spectra and FL lifetime can differentiate the metal ions (Cu(II) & Fe(III)).

In the present work, N-doped carbon (NCDs) dots with improved quantum yields were synthesized by a one-step hydrothermal method using o-phenylenediamine (OPD) and 2,5 pyridinedicarboxylic acid (2,5 PDC) as precursors. Excitation dependent emission nature of NCDs is decreased with increase in the pH. This supports the involvement of surface states in the origin of excitation dependent nature. Then the NCDs were employed as fluorescent probe for the simultaneous recognition of Fe(III) and Cu(II) ions. The emission intensity of NCDs can be selectively and rapidly diminished by both Fe(III) and Cu(II). With the addition of Cu(II), the

absorption spectra of NCDs presented a clear decrease in the intensity at 312 nm followed by an increase at 360 nm. This is not observed in the presence of Fe(III). In addition, the FL lifetime of NCDs is quenched by the presence of Fe(III) ions, whereas it remained constant with the addition of Cu(II). Thus, the simultaneous detection of both metals as well as their individual discrimination can be achieved without the help of any external reagent. The probe presented high selectivity for these two ions and further employed for the analysis of real samples.

## Experimental

### Materials

All the reagents and chemicals employed in the present study are of analytical quality, procured from SD Fine chemicals limited (<http://www.sdfine.com/home.aspx>), India and utilized without any additional refinement. All solutions were prepared by making use of double distilled (DD) water.

### Synthesis of nitrogen-doped carbon dots (NCDs)

Firstly, 108 mg of OPD is dissolved in 20 mL of DD water, then 167 mg of 2,5 PDC is added to the above solution, slowly with continuous stirring. After getting clear solution, it was transferred to a 25 mL of Teflon lined stainless steel autoclave which is then placed in an electric oven and heated at 180 °C for 5 h. After cooling down to room temperature naturally, the acquired solid product is dispersed in 10 mL of DD water by sonication. Then this NCDs solution is first centrifuged and then filtered by using 0.22 µm syringe filters to eliminate bulky particles. And the solution was purified by dialysing against DD water for one day using a dialysis tubing (MWCO 3500 Da). At last NCDs powder was achieved by freeze drying and specified quantity of the powder is dispersed in DD water to produce a solution of required concentration (1 mg mL<sup>-1</sup>) and for further use the solution is preserved in refrigerator.

### Fluorometric determination of metal ions

In this test all metal ion solutions were prepared from their respective salts using DD water. 50 µL of 0.1 mg mL<sup>-1</sup> NCDs solution is added to 2 mL of DD water and the FL intensity of this solution recorded at λ<sub>em</sub> = 406 nm (λ<sub>ex</sub> = 320 nm) is designated as F<sub>0</sub>. Likewise 50 µL of 0.1 mg mL<sup>-1</sup> NCDs solution is added to 2 mL of various metal ion solutions (50 µM). The solutions were jiggled and the FL intensity is recorded (λ<sub>em</sub> = 406 nm & λ<sub>ex</sub> = 320 nm) and designated as F. Similar procedure was followed for the sensitivity studies. Typically 50 µL

of 0.1 mg mL<sup>-1</sup> NCDs solution is mixed with 2 mL of metal ion solutions (Fe(III) or Cu(II)) of varying concentrations.

## Analysis of real samples

Waste, pond & bore water samples were collected respectively from a sewage, a small pond and hand pump bore well located in our university campus. These samples were centrifuged (12,000 rpm 10 min) and filtered (through 0.45 μ membrane filter) to rule out the interference of particulate matter. Human serum sample was obtained from Osmania General Hospital and centrifuged to remove the protein deposit. Urine samples were voluntarily collected from healthy individuals. Human serum and urine samples were diluted 100 times by phosphate buffered saline (containing 8 g NaCl, 0.2 g KCl, 1.44 g Na<sub>2</sub>HPO<sub>4</sub> and 0.24 g of KH<sub>2</sub>PO<sub>4</sub> in 1.0 L solution). These real samples (water, serum and urine) were spiked with metal ions (Fe(III) & Cu(II)) of desired concentrations. Then 50 μL of 0.1 mg mL<sup>-1</sup> NCDs solution is added to 2 mL of spiked real samples, shaken well and emission intensity is recorded ( $\lambda_{em} = 406$  nm &  $\lambda_{ex} = 320$  nm).

## Results and discussions

### Choice of materials

As mentioned earlier, various fluorescent probes including organic dyes, fluorescent metal nanoclusters and semiconductor quantum dots can be used for the detection of metal ions. However, they have flaws like cost of metal source, high toxicity, easy oxidation and photobleaching of the fluorescent dye [15]. In contrast, CDs present advantages like low cost, non-toxicity, high photostability and water solubility [21]. Moreover, their optical and surface chemical properties can be easily tuned by doping and surface functionalization. This can offer wide choice of probes for various analytes. Hence in the present work we have selected CDs tuned by doping with Nitrogen. We assume that the use of two nitrogen containing aromatic precursors created NCDs with specific response to two metal ions.

### Synthesis of NCDs

In this present scheme we employed a one-step hydrothermal approach for the synthesis of NCDs. As we aim to produce CDs with higher quantum yield (QY) values, and increased N content is known to enhance the QY, two nitrogen containing precursors were employed. Further to achieve CDs with high QY, synthetic conditions such as reaction temperature, time, and mole ratio of the reactants were optimized. As shown in the **Table S1** the NCDs synthesized by using 1:1 mol ratio of OPD and 2,5 PDC treated at 180 °C for 5 h exhibited highest

QY value of 47%. Furthermore, the effect of solution pH is also studied to understand the possible formation mechanism of NCDs. Interestingly, in slightly acidic medium NCDs were formed under mild reaction conditions (low temperature and less reaction time are sufficient to produce NCDs). However, strong acidic conditions resulted in the insoluble solid product which did not exhibit any detectable fluorescence. Whereas under basic conditions the reaction did not progressed (reaction mixture remained as non-fluorescent liquid) and NCDs were not formed. These results suggest that the polymerization of reactants via the creation of amide bond between COOH and NH<sub>2</sub> is the crucial step in the formation of NCDs. As acidic conditions will catalyse this polymerization reaction, mild reaction conditions can yield NCDs. whereas the amide bond formation is not favoured by base (base deprotonate COOH group and convert it to inactive COO<sup>-</sup> group), hence no reaction is observed under basic conditions. After polymerization, the produced oligomers will undergo carbonization to produce carbon dots. Possible formation mechanism for NCDs is represented in Scheme 1.

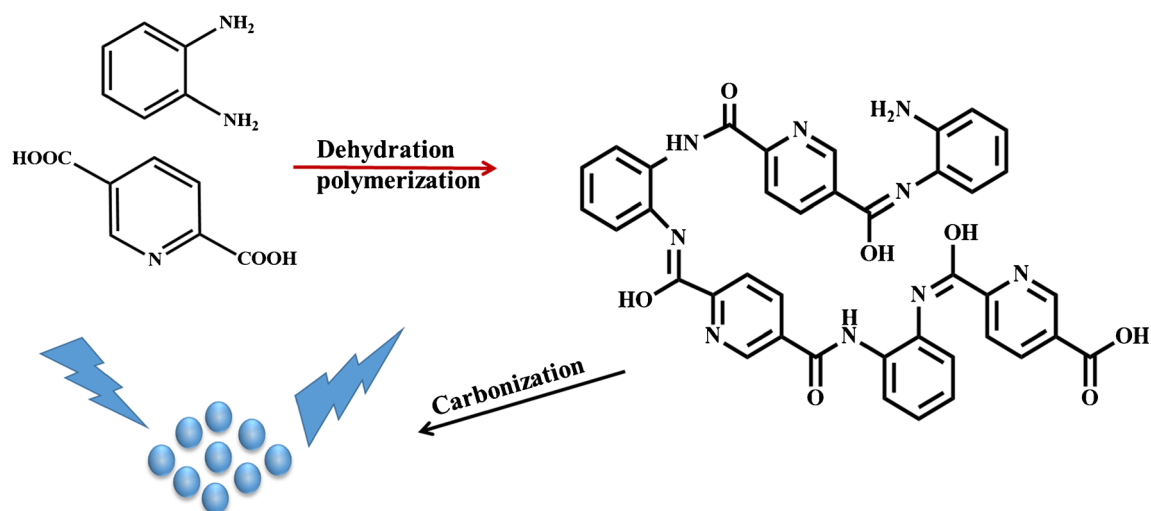
### Physicochemical properties

Morphological features and crystallinity/amorphous nature of NCDs are explored using Transmission electron microscopy (TEM), powder X-ray diffraction (XRD), and Raman spectroscopic analysis. Information related to chemical structure and surface functionalities is obtained from SEM-EDX, FT-IR and XPS analysis. Detailed explanation along with data is provided in [electronic supplementary material](#) (ESM).

### Optical properties

To gain an intuition into the optical properties, absorption and emission spectral examinations were conducted on NCDs aqueous solution at ambient conditions. UV-Vis spectra (black line in Fig. 1a) exhibit a wide absorption peak centred at about 312 nm, with a hump at around 280 nm. These two peaks can be assigned to  $n - \pi^*$  and  $\pi - \pi^*$  transitions respectively. Excitation spectra (red line) exhibit an intense peak at 320 nm and corresponding emission peak (blue line) is observed at 406 nm with a large stoke shift of 88 nm and a full width at half maximum (FWHM) of 65 nm. As shown in Fig. 1b, a gradual hike in the  $\lambda_{ex}$  from 260 nm to 370 nm caused fluctuations in the emission intensity along with a red shift in the emission wavelength. But unlike several previous reports [22, 23] the shift is very less. The QY of NCDs produced under optimal conditions is estimated by taking Quinine sulphate as reference compound is 47% (**Fig. S4**). This value is much higher than several previous reports [23–25] and can be ascribed to the usage of two nitrogen containing precursors.

Fluorescence stability studies (Refer ESM for complete details) revealed that NCDs possess great tolerance to high



**Scheme 1** Probable formation mechanism of N-doped carbon dots

ionic strength & continuous irradiation and have good shelf life (30 days).

### pH dependence

Influence of pH value on the optical properties of NCDs is studied by varying the solution pH from 2 to 12. Figure 2a represents the emission spectra of NCDs solution at various pH values recorded at an excitation of 320 nm. With increase in the pH, the emission intensity increased greatly, and reached to a maximum value at a pH of 7.5. Interestingly, this trend is accompanied by a clear blue shift in the maximum emission wavelength from 422 to 406 nm (Fig. 2b). In the pH range of 5 to 10 the emission wavelength almost remained constant but in the emission intensity small variation is recorded. However, further increase in the pH resulted in a clear red shift followed by a substantial decrease in the emission intensity. Further observation of emission peaks

revealed that the peaks in the pH range of 5 to 10 are more symmetrical with lower FWHM values (Fig. 2c) compared with those of strong acidic and basic. Corresponding absorption spectra of NCDs at varying pH is shown in Fig. 2d. Just like emission spectra, absorption spectra also not presented much changes in the pH range of 5–10. However, beyond this range two interesting features are observed. (1) Below this pH range, the hump at around 280 nm increased gradually with no changes in the peak at 312 nm. (2) Above the pH range, the hump at 280 nm is almost diminished and the peak at 312 nm presented a clear red shift. Effect of pH on the excitation dependence nature is also studied. Normalized emission spectra of NCDs under increasing  $\lambda_{\text{ex}}$  (from 270 to 370 nm, increment of 10 nm) at 3 different pH conditions i.e. strongly acidic (pH 3.05), neutral (pH 7.5) and strongly basic (pH 12.02) are shown in Fig. 3. The same at each pH value is shown in Fig. S6. Interestingly, commonly observed red shift in the emission peak position is

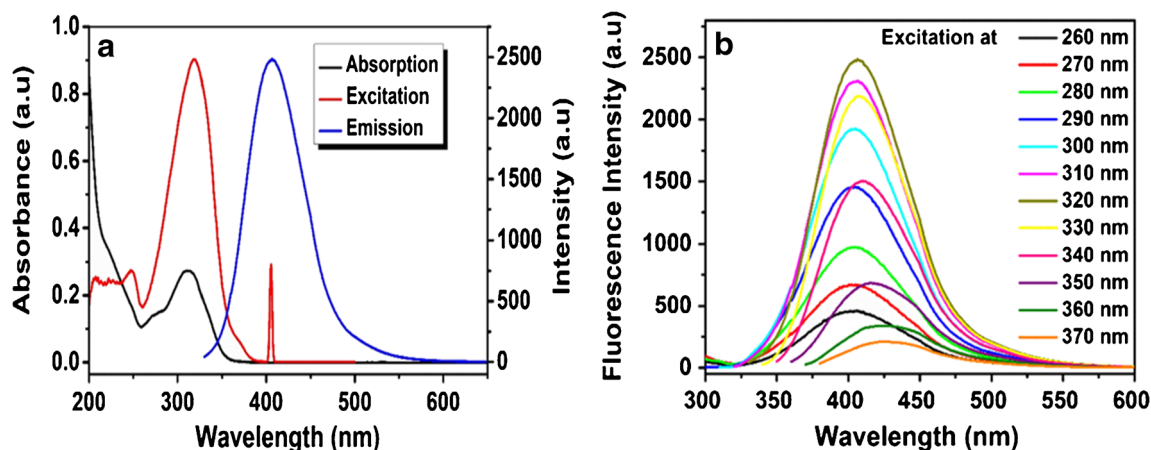


**Fig. 1** (a) Absorption (black), Excitation (red) and emission (blue) spectra of NCDs. (b) Emission spectra of NCDs at different excitation wavelengths as shown in the figure legend

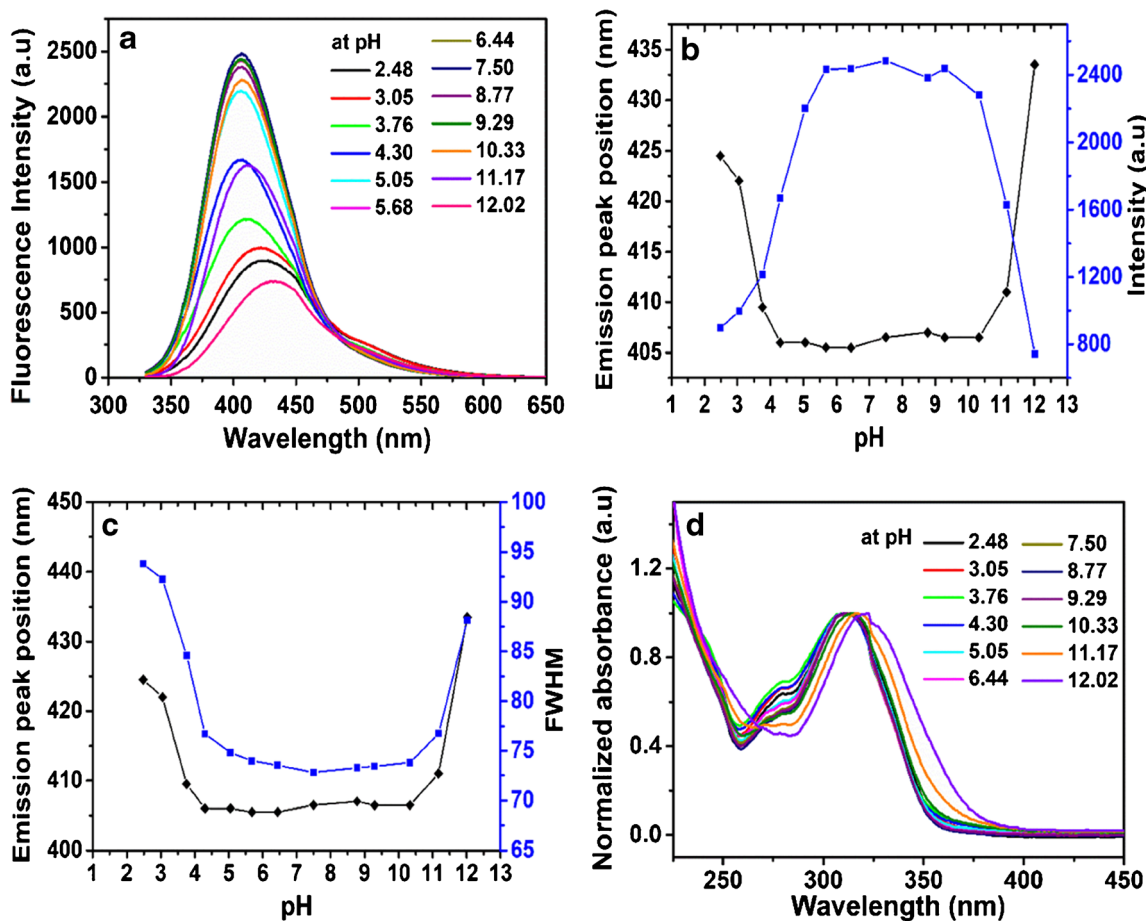


Fig. 2 (a) Emission spectra of NCDs at different pH values ( $\lambda_{ex} = 320$  nm) (b) Variation of emission peak position and intensity with pH ( $\lambda_{ex} = 320$  nm) (c) Variation of emission peak position and FWHM with pH ( $\lambda_{ex} = 320$  nm) (d) Normalized absorption spectra of NCDs at different pH values

also found to be pH dependent. With increase in the pH from 2 to 12, the red shift became less prominent. Clear red shift is observed only under strong acidic conditions, whereas the shift is insignificant under strong basic conditions.

Currently, the exact origin of this excitation tunable emission is unknown and there are several hypotheses starting from optical selection of differently sized particles to the presence of different emissive states and even to sluggish solvent relaxation around nanodot [26]. However, this kind of pH

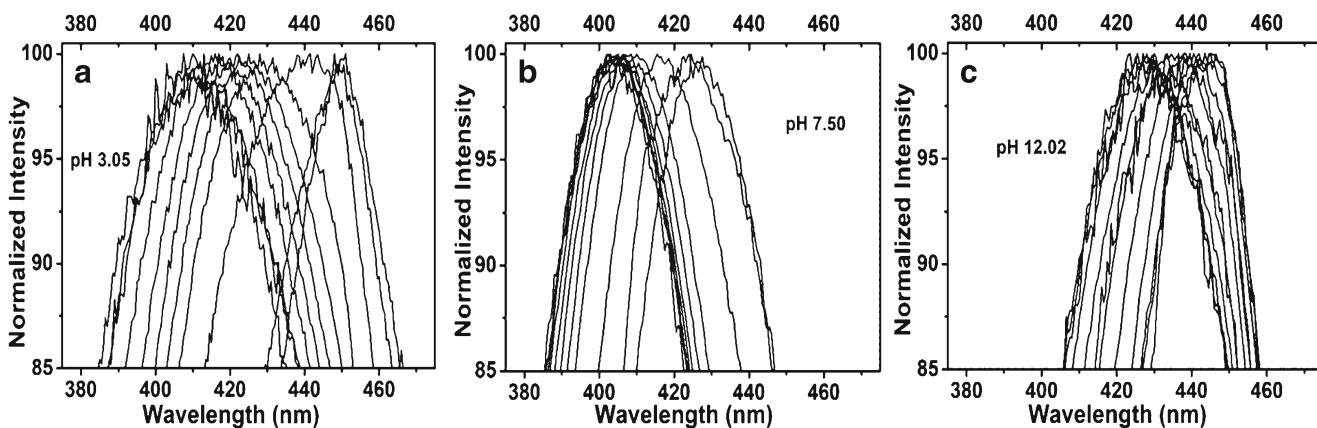
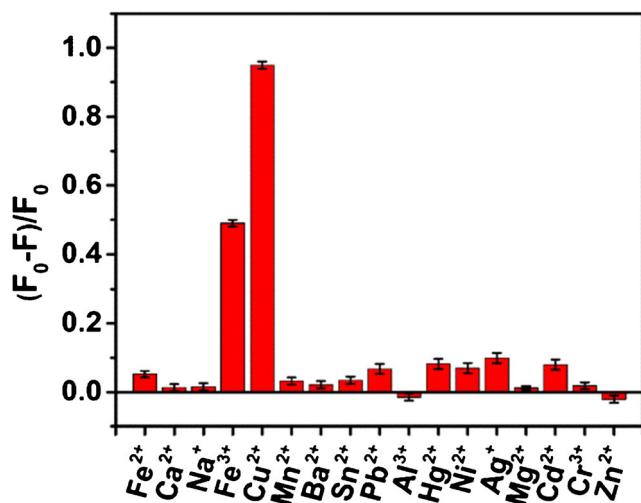


Fig. 3 Normalized emission spectra of NCDs under increasing excitation wavelengths ( $\lambda_{ex}$  from 270 to 370 nm, with increment of 10 nm) at (a) pH 3.05 (b) pH 7.50 (c) pH 12.02

dependence is quite rare. Based on the above results we have made some preliminary assumptions. The excitation dependent peak shift might be originated from surface inhomogeneity under acidic conditions, which is also evident from the broad emission peak (high FWHM) in acidic conditions. With increase in the pH, surface became homogeneous hence peak became narrow and less shift is observed. Increase in the emission intensity might be ascribed to the effective surface passivation caused by amine groups which are generally in the protonated form in acidic conditions. With increase in the pH un-protonated or free amine groups increases, which results in the increase in the emission intensity and surface homogeneity. The decrease in the emission intensity and red shift in the absorption & emission peak positions under strong basic conditions can be ascribed to the aggregation of nanoparticles by H – bond formation through hydroxyl ions. These assumptions are further supported by zeta potential and DLS size distribution analysis (Table S2). The interesting pH dependent nature of the absorption peak at 280 nm which is generally assigned to the  $\pi - \pi^*$  transition of the core state (considered to be shielded from external environment) can be related to the assumptions made by Arjun sharma et al. Accordingly, “the shielded core state, if true must be electronically well connected with the surface/edge functional groups to sample the changes in the external environment” [27].

### Fluorometric determination of metal ions

Impressed by their optical merits and wide surface functionalities, an attempt is made to explore their metal ions recognition capability. Figure 4 represents the fluorescence response ( $F_0 - F/F_0$ ) of NCDs to numerous biologically and environmentally important metal ions. Among all, NCDs exhibited great



**Fig. 4** Fluorescence responses ( $F_0 - F/F_0$ ) of NCDs towards various metal ions.  $F_0$  &  $F$  represent the emission peak intensities before and after the addition metal ions respectively ( $\lambda_{ex} = 320$  nm &  $\lambda_{em} = 406$  nm)

response to Cu(II) and Fe(III) ions, which unveiled their dual metal detecting capability.

What's more, some critical parameters such as the incubation time and pH of the solution are optimized to get the best detection performance. Incubation time of 1 min and pH range of 5–10 are found to be optimal for the detection of both metal ions. Respective data and figures are given in ESM.

Detection sensitivity of NCDs is evaluated by treating them with incremental amounts of metal ions (Cu(II) & Fe(III)). As evident from the Fig. 5a, the FL intensity at 406 nm decreased gradually with increasing the amount of Fe(III) ions in the scale of 0–90  $\mu$ M. The corresponding plot of FL response ( $F_0 - F/F_0$ ) vs Fe(III) concentration is shown in Fig. 5b. Linear relation ( $R^2 = 0.996$ ) is observed in the detection range of 3–60  $\mu$ M (Fig. 5c) and the correlation equation used to fit the data is

$$(F_0 - F/F_0) = 0.00976 * [\text{Fe(III)}]$$

Based the equation  $\text{LOD} = 3\sigma/m$  (where  $\sigma$  is the standard deviation of blank sample and  $m$  is slope of the linear fit), the limit of detection (LOD) for Fe(III) is found to be 0.31  $\mu$ M.

NCDs exhibited high response to Cu(II) ions, and the FL intensity is almost completely quenched by the addition of 25  $\mu$ M Cu(II) (Fig. 5d). The corresponding plot of FL response ( $F_0 - F/F_0$ ) vs Cu(II) concentration is shown in Fig. 5e. Excellent linear relation ( $R^2 = 0.998$ ) is observed (Fig. 5f) in the concentration range of 0.5–15  $\mu$ M with linear correlation equation

$$(F_0 - F/F_0) = 0.05273 * [\text{Cu(II)}]$$

The limit of detection (LOD) for Cu(II) calculated using the equation  $\text{LOD} = 3\sigma/m$  is found to be 56 nM. Analytical performance of our probe towards Fe(III) and Cu(II) is compared with various other related CDs based probes reported for Fe(III) or Cu(II) detection and furnished in Table 1. As can be observed, the probe offered by us has presented comparable linear range and relatively low LOD.

### Selectivity

As mentioned earlier, among several metal ions (50  $\mu$ M each) NCDs exhibited great response to only Fe(III) and Cu(II) ions, representing their excellent selectivity. However, for practical applicability, selectivity in the co-presence of high concentration of interfering metal ions is an important parameter. To test this, the FL response of NCDs towards Fe(III) and Cu(II) ions is recorded in the presence of extra added metal ions (200  $\mu$ M each) and the results are shown in Fig. 6. The black and red bars represent the FL response of Cu(II) and Fe(III) ions in the presence of extra added metal ions respectively. Blank indicates the presence of single metal ion (Cu(II) or Fe(III)). From

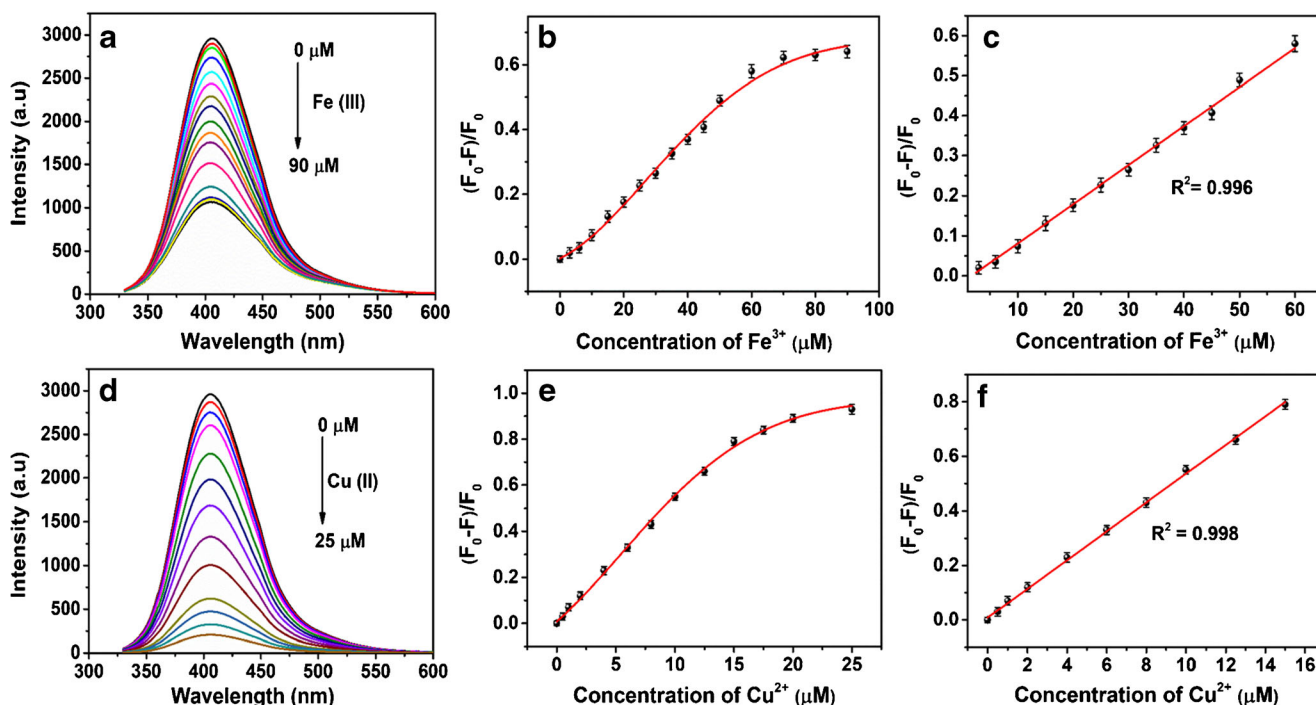


**Fig. 5** (a) Emission spectra ( $\lambda_{\text{ex}} = 320$  nm) of NCDs at different Fe(III) concentrations (0, 3, 6, 10, 15, 20, 25, 30, 35, 40, 45, 50, 60, 70, 80 & 90  $\mu\text{M}$ ) (b) plot of corresponding FL response ( $F_0-F/F_0$ ) vs Fe(III) concentration and (c) Linear fit ( $\lambda_{\text{ex}} = 320$  nm &  $\lambda_{\text{em}} = 406$  nm). (d) Emission spectra ( $\lambda_{\text{ex}} = 320$  nm) of NCDs at different

Cu(II) concentrations (0, 0.5, 1, 2, 4, 6, 8, 10, 12.5, 15, 17.5, 20 & 25  $\mu\text{M}$ ) (e) plot of corresponding FL response ( $F_0-F/F_0$ ) vs Cu(II) concentration and (f) Linear fit ( $\lambda_{\text{ex}} = 320$  nm &  $\lambda_{\text{em}} = 406$  nm).  $F_0$  &  $F$  represent the emission peak intensities before and after the addition metal ions respectively

the figure it is clear that no significant change in the FL response is observed in the presence of extra added metal ions, compared to that of Cu(II)/ Fe(III) alone. These outcomes obviously depict the highly selective nature of the present probe and further suggested their applicability to real sample analysis. This high selectivity can be attributed to (i) the special coordination between the electron rich surface functional (phenolic hydroxyl and/or amine) groups of NCDs with

electron deficient Fe(III) ions (which has been widely used for the detection of Fe(III) ions and color reactions in traditional organic chemistry) [23] & (ii) the specific interaction of Cu(II) ions with amino groups of NCDs to form cupric amine complex, which is also evident from the absorption spectra (Fig. 7a). However other metal ions can form only nonspecific

**Table 1** An overview on recently reported nanomaterial-based fluorometric methods for the determination of Fe(III) and Cu(II)

S.No.	Material	<sup>1</sup> LOD	Linear range	Ref
1	NCDs	Fe(III) 13.5 nM	0.05–30 $\mu\text{M}$	[3]
2	P,Cl-CDs	Fe(III) 0.06 $\mu\text{M}$	0.1–8.0 $\mu\text{M}$	[28]
3	CDs	Fe(III) 15 nM	0–30 $\mu\text{M}$	[29]
4	NCDs	Fe(III) 0.9 $\mu\text{M}$	2–25 $\mu\text{M}$	[30]
5	Rh6G/CDs	Fe(III) 0.727 $\mu\text{M}$	0–50 $\mu\text{M}$	[31]
6	NCDs	Fe(III) 0.31 $\mu\text{M}$	3–60 $\mu\text{M}$	This work
7	BNCds	Cu(II) 0.3 $\mu\text{M}$	1–25 $\mu\text{M}$	[32]
8	NCDs	Cu(II) 0.19 $\mu\text{M}$	0.6–30 $\mu\text{M}$	[4]
9	BCDs	Cu(II) 13.6 nM	0.05–300 $\mu\text{M}$	[33]
10	Cyclam-CDs	Cu(II) 100 nM	0.7–4 $\mu\text{M}$	[34]
11	CQDs	Cu(II) 0.0295 $\mu\text{M}$	0.25–10 $\mu\text{M}$	[35]
12	NCDs	Cu(II) 56 nM	0–15 $\mu\text{M}$	This work

<sup>1</sup> LOD = Limit of detection;

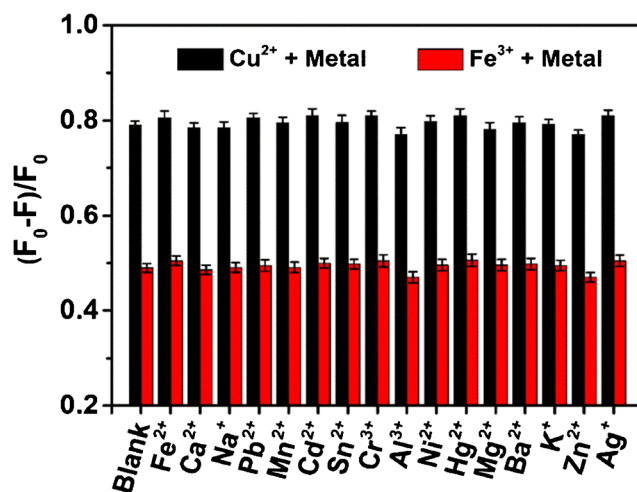


**Fig. 6** Fluorescence response ( $F_0-F/F_0$ ) of NCDs towards Cu(II) (black bars) and Fe(III) (red bars) in the co-presence of various metal ions.  $F_0$  &  $F$  represent the emission peak intensities before and after the addition metal ions respectively ( $\lambda_{\text{ex}} = 320$  nm &  $\lambda_{\text{em}} = 406$  nm)

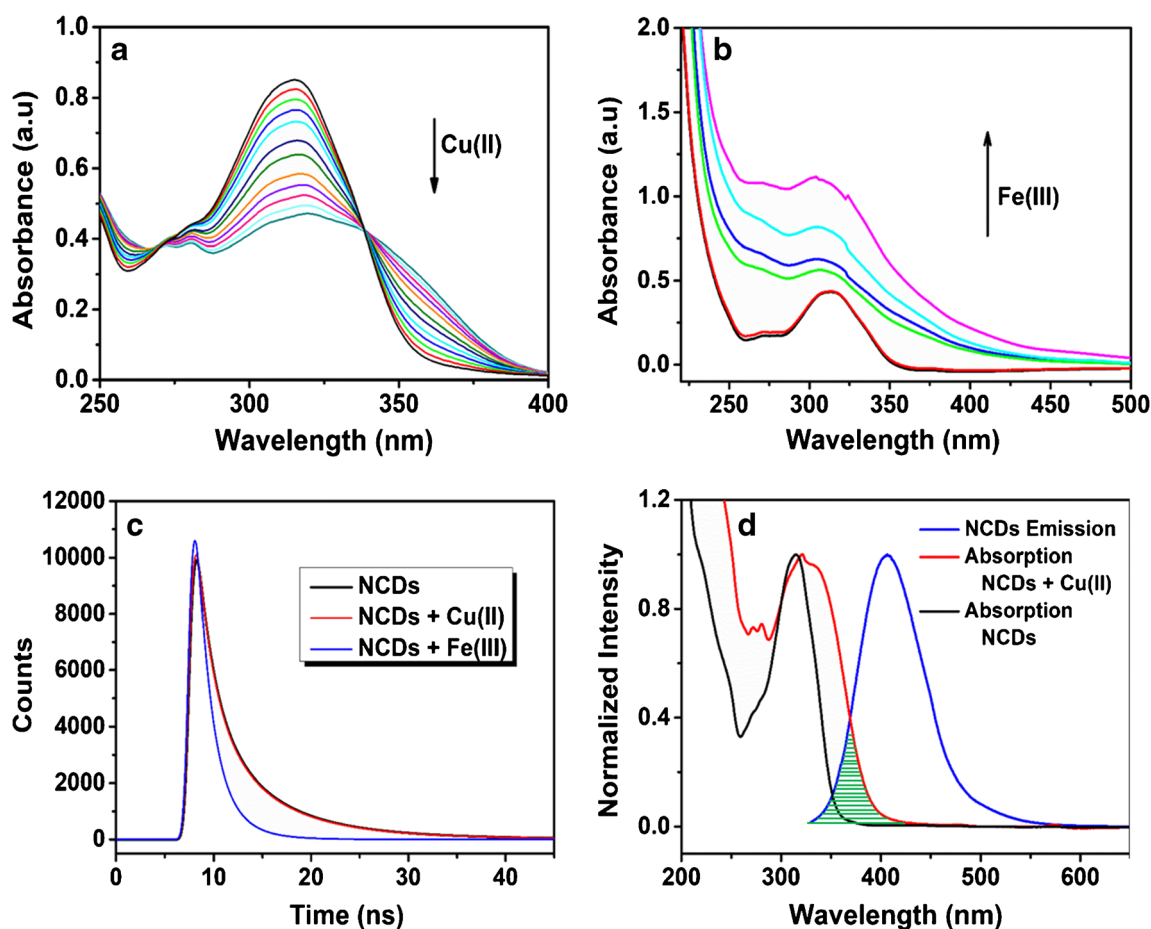


**Fig. 7** Absorption spectra of NCDs with increasing concentrations of (a) Cu(II) (b) Fe(III). (c) Fluorescence lifetime analysis of NCDs in the presence and absence of metal ions. (d) optical properties of NCDs and

NCDs/Cu(II) system showing significant overlap between the absorption spectra of NCDs/Cu(II) system and emission spectra of NCDs ( $\lambda_{\text{ex}} = 320 \text{ nm}$ )

interactions and hence they cannot produce significant interference even in excess amounts.

recognition of Fe(III) and Cu(II) in both environment and biological samples.

### Real sample analysis

Captivating analytical characteristics like high sensitivity, and selectivity stimulated us to further evaluate the detection efficiency of the NCDs probe in real samples. Three real water samples (pond, bore and waste water) and human serum and urine samples are employed for this purpose. The samples were spiked with different amounts of metal ions (Fe(III) & Cu(II)), analysed by the above described method. The recoveries achieved from their respective standard curves are presented in **Table S4** and **Table S5**. As depicted in the table, excellent recoveries (97% to 102%) with good RSD values ( $< 3$ ) are attained. The probe is further evaluated by analyzing the Fe(III) content in commercial ferrous sulfate tablets (Refer ESM for complete details). Further the probe is successfully employed for the simultaneous detection of two metal ions within the same sample (Refer ESM for complete details). All these results verified the potential of our probe for the

### Mechanism of detection and individual metal ion discrimination

To get some insight into the fluorescence quenching mechanism, we have first studied the changes in UV-Vis absorption spectra of NCDs with the addition of metal ions. Important observation is that the presence of Cu(II) can also be detected by analysing the UV-Vis spectra. With the addition of increasing concentrations of Cu(II) to NCDs aqueous solution, a gradual decrease in the absorption peak at 312 nm accompanied by a clear increase in the absorbance at 360 nm is observed (Fig. 7a). This change in the absorbance spectra can be attributed to the formation of copper amino and/or hydroxyl complex on the surface of NCDs. However, in the case of Fe(III) (Fig. 7b) only gradual increase in the intensity of absorption peak, which is due to the increased concentration Fe(III) is observed (Fe(III) will also have absorption in this region). This simple increase in the absorption rules out the



possibility of complex formation and support collisional quenching. To get deep into the quenching mechanism, FL lifetimes of NCDs were measured before and after the quenching process. As shown in the Fig. 7c, the FL lifetime of NCDs is decreased significantly with addition of Fe(III) clearly representing that the dynamic quenching is operating here. However the FL lifetime remained constant with the addition of Cu(II) indicating the static quenching involving the creation of non-fluorescent complex is operative here. Complex formation is further confirmed by UV-Vis spectra and raised the possibility of inner filter effect. As shown in the Fig. 7d the absorbance spectra of NCDs/Cu(II) system significantly overlaps with the emission spectrum of NCDs and further confirms the possibility of inner filter effect. Stern-Volmer plots are employed to further support our assumptions (Refer ESM for complete details). From all these results it is clear that both the metal ions produced distinct responses in both UV-Vis and FL lifetime analysis. Hence, the present method can be used for the simultaneous detection of Fe(III) & Cu(II) with individual metal ion differentiation without using any external masking agent.

## Limitations

Although NCDs presented many advantages, still there are some issues. For majority of the CDs, the excitation and/or emission wavelengths are limited to UV range [21]. This makes the probe prone to interference by UV absorbers. Blood, serum, cells, marine water, and waste water etc. always display strong background UV absorption. The UV light used for fluorescence excitation will be screened off by these UV absorbers and makes the signal weak. Similarly, the UV portion of emitted fluorescence will also be screened off. However, the effect of UV absorbers can be greatly reduced by simple pre-treatments like centrifugation, filtration and proper dilution of the sample. The second limitation of CDs is that the exact origin of their fluorescence and how the heteroatoms change their optical properties are unclear and still need further exploration.

## Conclusions

We have successfully demonstrated the hydrothermal production of greatly emissive NCDs with QY as high as 47%. The characteristic excitation tuneable emission behaviour of NCDs is found to be dependent on solution pH. This supports the involvement of surface states in the origin of excitation dependent nature. The NCDs applied as a fluorometric probe for the dual detection of Cu(II) and Fe(III). Individual discrimination of two metal ions is achieved by UV-Visible spectra and fluorescence lifetime analysis. Further the nano probe is successfully applied for the determination of Cu(II) and

Fe(III) ions in spiked real water, serum and urine samples. As the excitation and emission wavelengths are in the UV range, the probe is prone to interference by UV absorbers generally present in complex real samples. However, the effect of UV absorbers can be greatly reduced by simple pre-treatments like centrifugation, filtration and proper dilution of the sample. We hope our study stimulates the future research on CDs towards multi sensing applications where multiple analytes can be detected with single probe.

**Acknowledgements** One of the authors (Rajkumar Bandi) gratefully acknowledges CSIR-INDIA for Senior Research Fellowship. The authors are grateful to MRC, MNIT Jaipur for extending various analytical facilities. The authors would like to thank DST-FIST, New Delhi, India for providing necessary analytical facilities in the department. Sincere thanks to Department of Chemistry, Osmania University (OU) and CFRD-OU for providing infrastructure and other necessary facilities.

## Compliance with ethical standards

**Conflict of interest** There are no conflicts to declare.

**Ethical standards and informed consent** The urine sample was obtained from a healthy volunteer in Osmania University and informed consent was obtained for the use of human urine. Human serum sample was obtained from Osmania General Hospital (OGH) and appropriate permissions were taken from the relevant authorities of OGH for the use of human serum sample. This research was approved by Osmania University Ethical committee and all experiments were performed in accordance with the guideline for experimentation of Osmania University.

## References

1. Tapiero H, Townsend DM, Tew KD (2003) Trace elements in human physiology and pathology. Copper. *Biomed Pharmacother* 57: 386–398. [https://doi.org/10.1016/S0753-3322\(03\)00012-X](https://doi.org/10.1016/S0753-3322(03)00012-X)
2. Aisen P, Wessling-Resnick M, Leibold EA (1999) Iron metabolism. *Curr Opin Chem Biol* 3:200–206. [https://doi.org/10.1016/S1367-5931\(99\)80033-7](https://doi.org/10.1016/S1367-5931(99)80033-7)
3. Zhou X, Zhao G, Tan X et al (2019) Nitrogen-doped carbon dots with high quantum yield for colorimetric and fluorometric detection of ferric ions and in a fluorescent ink. *Microchim Acta* 186:67. <https://doi.org/10.1007/s00604-018-3176-9>
4. Zhao L, Li H, Xu Y et al (2018) Selective detection of copper ion in complex real samples based on nitrogen-doped carbon quantum dots. *Anal Bioanal Chem* 410:4301–4309. <https://doi.org/10.1007/s00216-018-1079-6>
5. Bandi R, Dadigala R, Gangapuram BR, Guttena V (2018) Green synthesis of highly fluorescent nitrogen – doped carbon dots from Lantana camara berries for effective detection of lead(II) and bioimaging. *J Photochem Photobiol B Biol* 178:330–338. <https://doi.org/10.1016/j.jphotobiol.2017.11.010>
6. Kou S, Nam SW, Shumi W et al (2009) Microfluidic detection of multiple heavy metal ions using fluorescent Chemosensors. *Bull Kor Chem Soc* 30:1173–1176. <https://doi.org/10.5012/bkcs.2009.30.5.1173>

7. Sun X, Lei Y (2017) Fluorescent carbon dots and their sensing applications. *TrAC - Trends Anal Chem* 89:163–180. <https://doi.org/10.1016/j.trac.2017.02.001>
8. Gao X, Du C, Zhuang Z, Chen W (2016) Carbon quantum dot-based nanoprobe for metal ion detection. *J Mater Chem C* 4:6927–6945. <https://doi.org/10.1039/c6tc02055k>
9. Gao W, Song H, Wang X et al (2018) Carbon Dots with Red Emission for Sensing of Pt 2+ , Au 3+ , and Pd 2+ and Their Bioapplications in Vitro and in Vivo. *ACS Appl Mater Interfaces* 10:1147–1154. <https://doi.org/10.1021/acsami.7b16991>
10. Zhu X, Wang J, Zhu Y et al (2018) Green emitting N,S-co-doped carbon dots for sensitive fluorometric determination of Fe(III) and Ag(I) ions, and as a solvatochromic probe. *Microchim Acta* 185: 510. <https://doi.org/10.1007/s00604-018-3045-6>
11. Ren G, Zhang Q, Li S et al (2017) One pot synthesis of highly fluorescent N doped C-dots and used as fluorescent probe detection for Hg<sup>2+</sup> and Ag<sup>+</sup> in aqueous solution. *Sensors Actuators B Chem* 243:244–253. <https://doi.org/10.1016/j.snb.2016.11.149>
12. Singh AK, Singh VK, Singh M et al (2019) One pot hydrothermal synthesis of fluorescent NP-carbon dots derived from Dunaliella salina biomass and its application in on-off sensing of Hg (II), Cr (VI) and live cell imaging. *J Photochem Photobiol A Chem* 376: 63–72. <https://doi.org/10.1016/j.jphotochem.2019.02.023>
13. Zhang S, Li J, Zeng M et al (2014) Polymer nanodots of graphitic carbon nitride as effective fluorescent probes for the detection of Fe<sup>3+</sup> and Cu<sup>2+</sup> ions. *Nanoscale* 6:4157–4162. <https://doi.org/10.1039/c3nr06744k>
14. Wang B, Tan H, Zhang T et al (2019) Hydrothermal synthesis of N-doped carbon dots from an ethanolamine-ionic liquid gel to construct label-free multifunctional fluorescent probes for Hg 2+ , Cu 2+ and S 2 O 3 2-. *Analyst* 144:3013–3022. <https://doi.org/10.1039/c9an00116f>
15. Patir K, Gogoi SK (2019) Nitrogen-doped carbon dots as fluorescence ON–OFF–ON sensor for parallel detection of copper( ii ) and mercury( ii ) ions in solutions as well as in filter paper-based microfluidic device. *Nanoscale Adv* 1:592–601. <https://doi.org/10.1039/c8na00080h>
16. Yu J, Song N, Zhang Y-K et al (2015) Green preparation of carbon dots by Jinhua bergamot for sensitive and selective fluorescent detection of Hg<sup>2+</sup> and Fe<sup>3+</sup>. *Sensors Actuators B Chem* 214:29–35. <https://doi.org/10.1016/j.snb.2015.03.006>
17. Ye Q, Yan F, Luo Y et al (2017) Formation of N, S-codoped fluorescent carbon dots from biomass and their application for the selective detection of mercury and iron ion. *Spectrochim Acta - Part A Mol Biomol Spectrosc* 173:854–862. <https://doi.org/10.1016/j.saa.2016.10.039>
18. Li C, Liu W, Ren Y et al (2017) The selectivity of the carboxylate groups terminated carbon dots switched by buffer solutions for the detection of multi-metal ions. *Sensors Actuators B Chem* 240:941–948. <https://doi.org/10.1016/j.snb.2016.09.068>
19. Luo L, Wang P, Wang Y, Wang F (2018) pH assisted selective detection of Hg(II) and Ag(I) based on nitrogen-rich carbon dots. *Sensors Actuators B Chem* 273:1640–1647. <https://doi.org/10.1016/j.snb.2018.07.090>
20. Sharma V, Saini AK, Mobin SM (2016) Multicolour fluorescent carbon nanoparticle probes for live cell imaging and dual palladium and mercury sensors. *J Mater Chem B* 4:2466–2476. <https://doi.org/10.1039/C6TB00238B>
21. Roy P, Chen PC, Periasamy AP et al (2015) Photoluminescent carbon nanodots: synthesis, physicochemical properties and analytical applications. *Mater Today* 18:447–458. <https://doi.org/10.1016/j.mattod.2015.04.005>
22. Ramanan V, Thiyagarajan SK, Raji K et al (2016) Outright green synthesis of fluorescent carbon dots from eutrophic algal blooms for in vitro imaging. *ACS Sustain Chem Eng* 4:4724–4731. <https://doi.org/10.1021/acssuschemeng.6b00935>
23. Bandi R, Gangapuram BR, Dadigala R et al (2016) Facile and green synthesis of fluorescent carbon dots from onion waste and their potential applications as sensor and multicolour imaging agents. *RSC Adv* 6:28633–28639. <https://doi.org/10.1039/c6ra01669c>
24. Ramanan V, Siddaiah B, Raji K, Ramamurthy P (2018) Green synthesis of multifunctionalized, nitrogen-doped, highly fluorescent carbon dots from waste expanded polystyrene and its application in the Fluorimetric detection of Au<sup>3+</sup> ions in aqueous media. *ACS Sustain Chem Eng* 6:1627–1638. <https://doi.org/10.1021/acssuschemeng.7b02852>
25. Bandi R, Devulapalli NP, Dadigala R et al (2018) Facile Conversion of Toxic Cigarette Butts to N,S-Codoped Carbon Dots and Their Application in Fluorescent Film, Security Ink, Bioimaging, Sensing and Logic Gate Operation. *ACS Omega* 3: 13454–13466. <https://doi.org/10.1021/acsomega.8b01743>
26. Sharma A, Gadly T, Gupta A et al (2016) Origin of excitation dependent fluorescence in carbon Nanodots. *J Phys Chem Lett* 7: 3695–3702. <https://doi.org/10.1021/acs.jpcclett.6b01791>
27. Sharma A, Gadly T, Neogy S et al (2017) Molecular origin and self-assembly of fluorescent carbon Nanodots in polar solvents. *J Phys Chem Lett* 8:1044–1052. <https://doi.org/10.1021/acs.jpcclett.7b00170>
28. Wang W, Peng J, Li F et al (2019) Phosphorus and chlorine codoped carbon dots with strong photoluminescence as a fluorescent probe for ferric ions. *Microchim Acta* 186:32–39. <https://doi.org/10.1007/s00604-018-3140-8>
29. Sun Y, Wang X, Wang C et al (2018) Red emitting and highly stable carbon dots with dual response to pH values and ferric ions. *Microchim Acta* 185:83. <https://doi.org/10.1007/s00604-017-2544-1>
30. Atchudan R, Edison TNJI, Aseer KR et al (2018) Highly fluorescent nitrogen-doped carbon dots derived from Phyllanthus acidus utilized as a fluorescent probe for label-free selective detection of Fe<sup>3+</sup> ions, live cell imaging and fluorescent ink. *Biosens Bioelectron* 99:303–311. <https://doi.org/10.1016/j.bios.2017.07.076>
31. Deng M, Wang S, Liang C et al (2016) A FRET fluorescent nanosensor based on carbon dots for ratiometric detection of Fe 3+ in aqueous solution. *RSC Adv* 6:26936–26940. <https://doi.org/10.1039/c6ra02679f>
32. Rong MC, Zhang KX, Wang YR, Chen X (2017) The synthesis of B, N-carbon dots by a combustion method and the application of fluorescence detection for Cu 2+. *Chin Chem Lett* 28:1119–1124. <https://doi.org/10.1016/j.ccllet.2016.12.009>
33. Wang ZX, Yu XH, Li F et al (2017) Preparation of boron-doped carbon dots for fluorometric determination of Pb(II), Cu(II) and pyrophosphate ions. *Microchim Acta* 184:4775–4783. <https://doi.org/10.1007/s00604-017-2526-3>
34. Chen J, Li Y, Lv K et al (2016) Cyclam-functionalized carbon dots sensor for sensitive and selective detection of copper(II) ion and sulfide anion in aqueous media and its imaging in live cells. *Sensors Actuators B Chem* 224:298–306. <https://doi.org/10.1016/j.snb.2015.10.046>
35. Wang Y, Wu WT, Wu MB et al (2015) Yellow-visual fluorescent carbon quantum dots from petroleum coke for the efficient detection of Cu<sup>2+</sup> ions. *Xinxing Tan Cailiao/New Carbon Mater* 30: 550–559. [https://doi.org/10.1016/S1872-5805\(15\)60204-9](https://doi.org/10.1016/S1872-5805(15)60204-9)

**Publisher's note** Springer Nature remains neutral with regard to jurisdictional claims in published maps and institutional affiliations.